

## EFFECT OF Ni-DOPING ON THE STRUCTURAL AND OPTICAL PROPERTIES OF ZnO NANOPARTICLES PREPARED BY CHEMICAL PRECIPITATION METHOD

D. TAMILSELVI<sup>a,b,\*</sup>, N. VELMANI<sup>c</sup>, K. RATHIDEVI<sup>a,d</sup>

<sup>a</sup>Research & Development Centre, Bharathiar University, Coimbatore – 641 046, Tamilnadu, India

<sup>b</sup>Assistant Professor, Department of Science and Humanities, Rathinam Technical Campus, Coimbatore – 641 021, Tamilnadu, India

<sup>c</sup>Assistant Professor, Department of Chemistry, Government arts College, Coimbatore -641 018, Tamilnadu, India

<sup>d</sup>Assistant Professor, Department of Science and Humanities, Kumaraguru College of Technology, Coimbatore – 641 049, Tamilnadu, India

Undoped ZnO nano particles and Ni doped ZnO nanoparticles prepared by chemical precipitation method and assessed for their structural, morphological and optical properties. The prepared undoped and Ni doped ZnO nanoparticles were characterized by using X-ray diffraction (XRD), Fourier transform infrared spectral (FTIR), UV-Visible spectrophotometer, Scanning electron microscopy (SEM) and Energy Dispersive X-ray analysis (EDAX), Photoluminescence spectra (PL). XRD pattern shows the purity of prepared undoped and Ni doped ZnO nanoparticles size. Scanning electron microscopy (SEM) observations revealed remarkable change in morphology of the prepared samples. The presence of functional groups and chemical bonding was confirmed by FTIR and UV analysis. The defect states were revealed from the UV and visible emissions of the photoluminescence spectra.

(Received December 12, 2019; Accepted April 2, 2020)

*Keywords:* ZnO, Ni - ZnO, XRD, SEM, Chemical precipitation method

### 1. Introduction

Nanoparticles have attracted very much interest in the research field due to their performance in different applications such as electronics, optics, and photonics and excellent optimized properties. Based on the dimensional nanoparticles are classified into three groups: 0-dimensional, 1-dimensional, and 2-dimensional nanostructures. The various semiconductors (e.g.: ZnO, TiO<sub>2</sub>, WO<sub>3</sub>, SnO<sub>2</sub>, ZnS, ZnSe, CdS, GaP, GaAs, etc.) are used in different application field. Such as optoelectronics, catalysis, solar cells, ultraviolet light emitter, piezoelectric device, chemical gas sensors etc<sup>[1-6]</sup>. Among these all the semiconductors, ZnO nanoparticles have used in different application field such as biomedical, charge behavior, catalytic reactions, glucose biosensors, pathogenic microorganisms, water treatment etc<sup>[7-12]</sup>. Zinc oxide is a nontoxic, low cost and excellent semiconductor nanomaterial with wide band gap of 3.37eV and large excitation binding energy of 60 meV<sup>13,14</sup>. ZnO nanomaterials having a lot of morphology structures have been reported such as nano-combs<sup>15, 16</sup>, nanotubes<sup>17</sup>, nano-springs<sup>18</sup>, nanorods<sup>19</sup>, nanorings<sup>20</sup>, nanowires<sup>21</sup> and nanoflower<sup>22</sup>, due to their physical and chemical properties of crystals. Transition metals (such as: Ni, CO, Mn, Cr, Fe) doped with ZnO nanomaterial to obtain dilute magnetic semiconductors (DMS). These transition metals improve the electrical, optical and magnetic properties<sup>23-24</sup>. DMS used in spintronics devices<sup>[25-29]</sup>. The doping concentration of the metal with ZnO and calcination process induces some changes in the structure, physical and chemical properties of prepared nanomaterials (ZnO). Some of the dopants, Ni is one of the most favorable transition metal for amalgamate with ZnO, due to their valence, ionic radii are closer to that of

\* Corresponding author: tamilselviupdate@gmail.com

Zn<sup>2+</sup>. So Zn<sup>2+</sup> replaced by Ni<sup>2+</sup> which gives high donor effect, charge separation and transport in the ZnO nanostructure. Ni doped ZnO nano material is used in several application fields, such as spintronics<sup>28, 29</sup>, photo-electronics devices<sup>30, 31</sup>, nano-sensors<sup>32-34</sup>, nano-generators, electronics devices, dye-sensitized solar cells, metal-ions detection, photo-catalytic, field emission devices, antifungal activity etc. Ni doped ZnO nanoparticles were prepared by various methods such as RF Sputtering, thermal evaporation wet chemical, reflux, hydro thermal, chemical Co-precipitation, solvothermal, Sol gel, Spin coating techniques have also been reported by many researchers. In this present work ZnO and Ni doped ZnO nanoparticles has been prepared by chemical Co-precipitation method. The calcinated power samples were studied by XRD, FTIR, SEM, EDAX, UV, PL and the results of their structural, morphological and optical properties has been discussed.

## 2. Experimental details

### 2.1. Materials

The high purity chemicals (>99% purity) such as Zinc chloride (ZnCl<sub>2</sub>), Nickel Chloride (NiCl<sub>2</sub>) and Sodium Hydroxide (NaOH) were purchased from Sd. Fine chemicals (AR) grade and used were used as the precursors without further purification.

### 2.2. Synthesis of ZnO and Ni doped ZnO nanoparticles.

For the preparation of Zn<sub>1-x</sub>Ni<sub>x</sub>O samples were synthesized by chemical CO-precipitation method<sup>49</sup>. Ni doped ZnO samples were prepared with different Ni compositions of x = 0, 0.02, 0.04 and 0.06 mol respectively. To synthesis pure ZnO, 0.1M Zinc chloride was dissolved in 100ml double distilled water and kept in magnetic stirrer for 10 mins under vigorous stirring (solution A). 0.3M NaOH solution was then added drop wise into the initial aqueous solution (A) under constant stirring up to 2hrs to reach the p<sup>H</sup> value of 12. The formed gelatinous white precipitates were filtered and washed with distilled water, ethanol, dry for overnight at room temperature and dried in oven at 100° C for six hours. The dried white precipitates then annealed at 500° C for two hours followed by grinding to get fine particles. These were used for various characterization techniques. The same procedure was repeated to prepare Ni doped ZnO samples by Zinc chloride (0.1M) and Nickel Chloride(0.1M) were dissolved in 100 ml double distilled water solution (A) and 0.3 M NaOH was prepared in 100 ml double distilled water then added drop wise into the initial aqueous solution (A) constant stirring up to 2hrs to reach the p<sup>H</sup> value of 12. The formed green precipitates were filtered and washed with distilled water, ethanol, dry for overnight at room temperature and dried in oven at 100° C for six hours. The dried green precipitates then annealed at 500° C for two hours followed by grinding to get fine particles. These were used for various characterization techniques [15-21].

## 3. Characterization techniques

All the synthesized nano particles has been characterized at room temperature by X-ray powder diffraction (XRD) with Philips Analytical Model: X'Pert PRO equipped with CuK $\alpha$  radiation  $\lambda = 1.54187 \text{ \AA}$  and operating rate of 1°/min at 40 kV/30mA. The Scanning angle range  $2\theta$  between 30 - 90° was maintained. The powder samples have been examined with Fourier Transform Infrared Spectrometer (FTIR) to identify the functional groups and to confirm the presence Ni<sup>2+</sup> ions with the measurements range recorded in the region 400 – 4000 cm<sup>-1</sup>. The optical studies of Photoluminescence (PL) spectrum recorded from 350 nm to 500 nm. The absorption studies recorded by UV-visible spectro-photometer from 100 to 900 nm. The structure and Surface morphology of the particles also have been examined using (HR-SEM) HR-field emission scanning electron operated at 10kV. The synthesized nanoparticles have been examined with Energy-Dispersive X-ray Spectrometer (EDAX) to identify elemental composition analysis.

## 4. Results and discussion

### 4.1 XRD Structural analysis

Fig. 1. Shows the XRD diffraction patterns of Zinc oxide and Ni-doped ZnO nanoparticles of  $x = 0, 0.02, 0.04$  and  $0.06$  mol. The XRD patterns of pure ZnO nanoparticles clearly shows the crystalline nature and well-defined sharp diffraction peaks corresponding to (100), (002), (101), (111), (102), (110), (103), (112), and (203) planes were observed for all the samples.

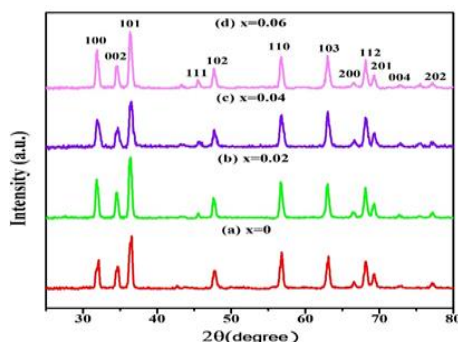


Fig. 1. XRD of synthesized  $Zn_{1-x}Ni_xO$  ( $x = 0, 0.02, 0.04$  and  $0.06$ ) nanoparticles annealed at  $500^\circ C$ .

The standard diffraction peaks clearly show the crystallize in the hexagonal wurtzite structure with space group  $P6_3mc, 186$ . All the peaks match well with the JCPDS data card No. 36-1451. The peaks with preferred orientation along (101) plane in all the samples. No characteristic addition peaks corresponding to Ni and NiO were observed, which indicates no impurities or secondary phase exist in the samples. This is most stable single phase of synthesized ZnO products, as well as the possible substitution of  $Ni^{2+}$  into ZnO lattice, shows an additional XRD peaks appears at diffraction angle( $2\theta$ ) of  $43.7$  and  $51.9$  corresponding to (111) and (200) planes. Therefore NiO phase was confirmed by the substitutional limit for doping Ni ions in ZnO. The standard diffraction peaks clearly show the crystallize in the cubic structure with space group  $F3-3m, 225$ , these two peaks match well with the JCPDS data card No. 01-1239. A small shift towards the higher angle( $2\theta$ ) was observed with an increase in Ni doped concentration of ZnO when compared to ZnO. This is due to the filling of Ni ions in Zn sites. The average crystallite size was calculated by using De-bye-Scherrer formula,

$$D = 0.94\lambda / \beta \cos(\theta), \text{ where } D - \text{average crystallite size, } \lambda - \text{wavelength (1.5406 \AA)},$$

$\beta$  – FWHM (full width at half maximum of individual peak at  $2\theta$ ,  $\theta$  – Bragg angle.

The average crystallite size was predicted to be 24-35 nm for synthesized  $Zn_{1-x}Ni_xO$  ( $x = 0, 0.02, 0.04$  and  $0.06$ ) nanoparticles annealed at  $500^\circ C$ . The increase in particle size observed here with the increase in Ni concentration. This is due to doping level of Ni in ZnO nanoparticles [31-34].

Table 1. The Average particle Size of synthesized  $Zn_{1-x}Ni_xO$  ( $x = 0, 0.02, 0.04$  and  $0.06$ ) nanoparticles annealed at  $500^\circ C$  using X-ray diffraction spectra.

Sample code (weight %)	Average Crystallite size (D) nm
(a) ZnO	24
(b) $Zn_{0.98}Ni_{0.02}O$	25
(c) $Zn_{0.96}Ni_{0.04}O$	29
(d) $Zn_{0.94}Ni_{0.06}O$	35

#### 4.2. Fourier transform infrared spectroscopy (FTIR) - Analysis

The chemical bonding and constituting elements in the samples can be analyzed by using FTIR spectrum. Fig. 2 shows FTIR spectra of all the samples of  $Zn_{1-x}Ni_xO$  are recorded in the range  $4000 - 400\text{ cm}^{-1}$ . The absorption peak around  $456\text{ cm}^{-1}$  corresponds to ZnO stretching vibrations [22] and that around  $2308 - 2390\text{ cm}^{-1}$  is assigned to the Ni-CO stretching [23,24] for all the samples. The other broad absorption peaks observed in all the samples around  $3609\text{ cm}^{-1}$  and  $1693\text{ cm}^{-1}$  due to O-H stretching of water molecule and bending vibrations of O-H molecule respectively [55,56]. The peaks at  $2926\text{ cm}^{-1}$  and  $2308\text{ cm}^{-1}$  corresponds to C-H stretching vibrations [25-28] and O = C = O symmetric stretching vibrations modes [60]. The peaks at  $1514\text{ cm}^{-1}$  due to antisymmetric stretching vibrations of  $(COO^-)$  respectively have their adsorbed compounds on the surface of the sample [29].

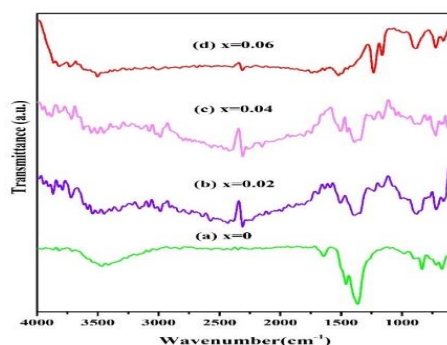


Fig. 2. FTIR spectra of synthesized  $Zn_{1-x}Ni_xO$  ( $x = 0, 0.02, 0.04$  and  $0.06$ ) nanoparticles annealed at  $500\text{ }^\circ\text{C}$ .

#### 4.3 SEM Analysis

The Surface morphology of synthesized  $Zn_{1-x}Ni_xO$  nanoparticles were shown in the fig. from 3(a-d). The SEM images of pure ZnO featured a flower like nano structure shows in fig 3(a). 2,4 and 6 % of Ni doped ZnO nanoparticles featured a Nano rod like nano structures shows from fig 3(b) to 3(d) because of particles are more agglomerated due to increase in doping concentration.

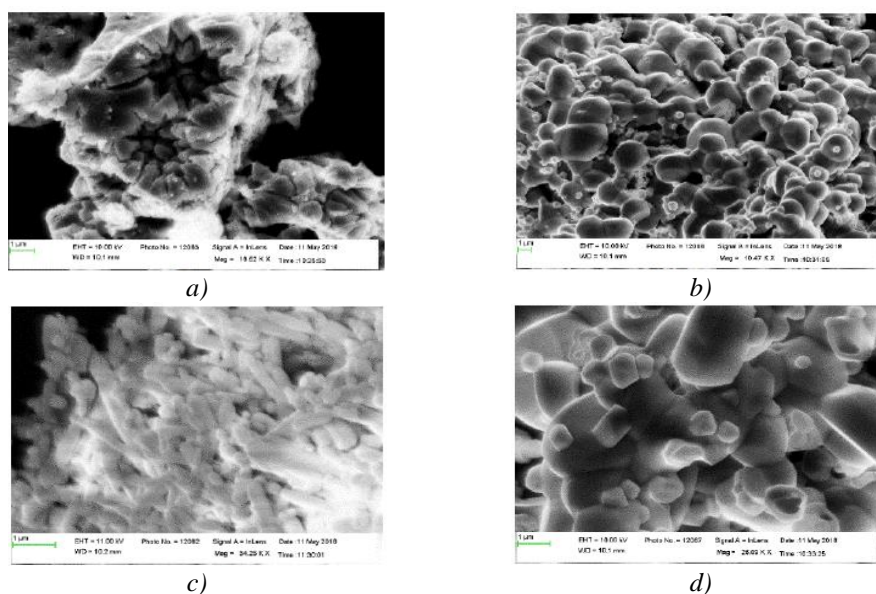


Fig. 3. SEM image of synthesized  $Zn_{1-x}Ni_xO$  nanoparticles annealed at  $500\text{ }^\circ\text{C}$ : a)  $X=0$ ; b)  $X=0.02$ ; c)  $X=0.04$ ; d)  $X=0.06$

#### 4.4. EDAX ANALYSIS

Fig. 4. Shows the elemental composition of the synthesized  $Zn_{1-x}Ni_xO$  ( $x = 0, 0.02, 0.04$  and  $0.06$ ) nanoparticles were measured by EDAX analysis. From this spectrum, the elements of Zn, Ni, O, and C present in the samples. The C peaks corresponds to their origin in copper grid. EDAX spectrum shows no impurities present in the synthesized  $Zn_{1-x}Ni_xO$  samples. The data of weight and atomic percentage of element were also confirmed by EDAX spectrum and presented in table 2.

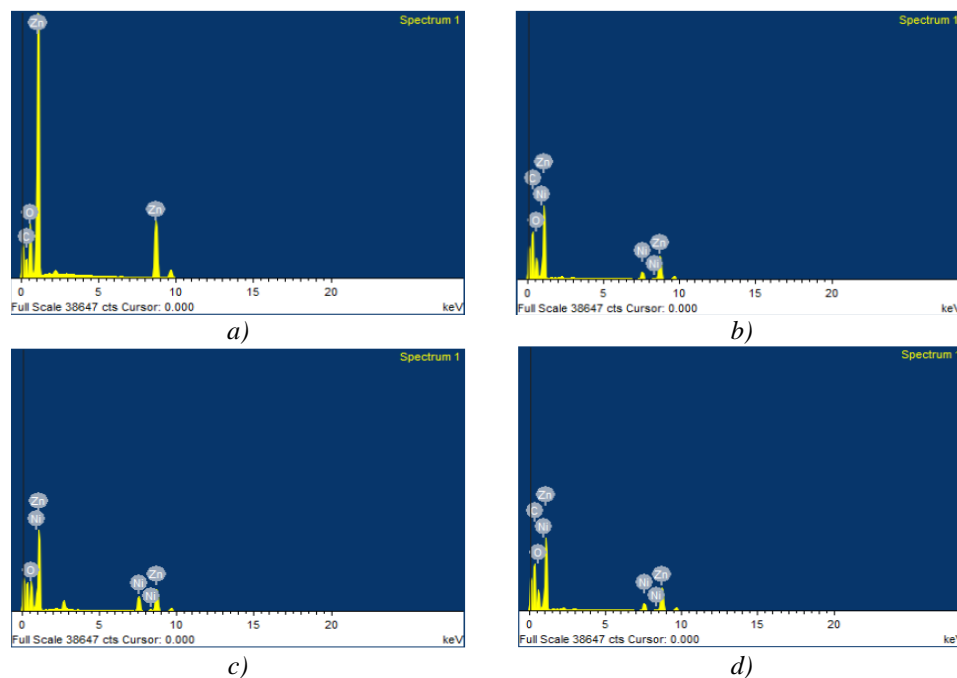


Fig. 4. EDAX spectra of synthesized  $Zn_{1-x}Ni_xO$  nanoparticles annealed at  $500\text{ }^{\circ}\text{C}$ : a)  $X=0$ ; b)  $X=0.02$ ; c)  $X=0.04$ ; d)  $X=0.06$

Table 2. Weight percentage of synthesized  $Zn_{1-x}Ni_xO$  nanoparticles from EDAX spectrum.

Samples	Zn Wt. %	Ni Wt. %	O Wt. %	Ni/Zn Wt. % ratio
ZnO	71.91	-	28.09	-
$Zn_{0.08}Ni_{0.02}O$	71.48	1.37	27.15	0.019
$Zn_{0.06}Ni_{0.04}O$	70.99	2.75	26.26	0.038
$Zn_{0.04}Ni_{0.06}O$	70.69	4.12	25.19	0.058

#### 4.5. UV-Vis spectral Analysis

The optical absorption spectra of the synthesized  $Zn_{1-x}Ni_xO$  ( $x = 0, 0.02, 0.04$  and  $0.06$ ) nanoparticles was shown in Fig 5. Generally, the position of absorbance value is depends on the size of the nanoparticles, oxygen deficiency, grain structure, band gap etc. The absorption peak of the ZnO nanoparticles appeared at 371 nm. The absorption peak appeared at 379nm, 382nm, 383nm for the doped samples of the synthesized  $Zn_{1-x}Ni_xO$  ( $x = 0.02, 0.04$  and  $0.06$ ) nanoparticles respectively. The excitonic peaks clearly shows red shift for Ni doped samples. Absorption spectra of Ni doped ZnO nanoparticles shows that the absorption peak value is slightly shifted towards the longer wavelength (red shift) when compared to undoped ZnO nanoparticles. The shift of the absorption peak value to the longer wavelength is due to the small increase of particle size with increasing Ni concentration. The optical band gap value was shown in Fig 6., as 3.37eV, 3.32eV,

3.29 eV and 3.0 eV for the synthesized  $Zn_{1-x}Ni_xO$  ( $x = 0.02, 0.04$  and  $0.06$ ) nanoparticles respectively (30-33).

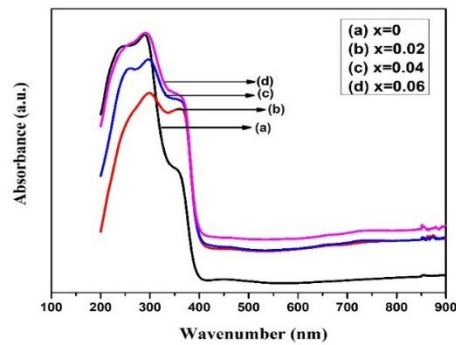


Fig. 5. UV-Vis spectra of synthesized  $Zn_{1-x}Ni_xO$  ( $x = 0, 0.02, 0.04$  and  $0.06$ ) nanoparticles annealed at  $500^\circ C$ .

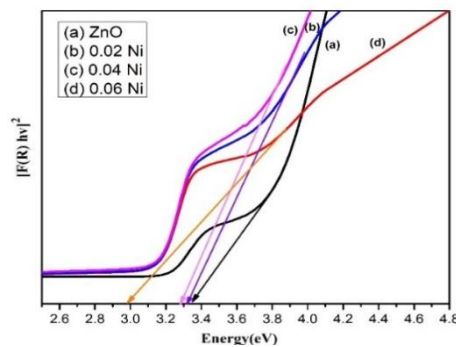


Fig. 6. Band gap spectra of synthesized  $Zn_{1-x}Ni_xO$  ( $x = 0, 0.02, 0.04$  and  $0.06$ ) nanoparticles annealed at  $500^\circ C$ .

#### 4.6. PL spectra analysis

The PL spectra of synthesized  $Zn_{1-x}Ni_xO$  ( $x = 0, 0.02, 0.04$  and  $0.06$ ) nanoparticles was shown in Fig 7. The PL spectra shows emission peak around 391 nm for both undoped and Ni-doped ZnO nanoparticles corresponding to UV emissions due to near band gap excitonic emission process.

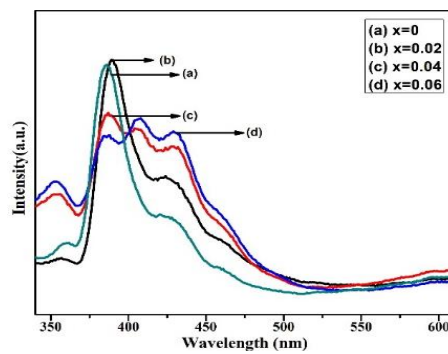


Fig. 7. PL spectra of synthesized  $Zn_{1-x}Ni_xO$  ( $x = 0, 0.02, 0.04$  and  $0.06$ ) nanoparticles annealed at  $500^\circ C$ .

The strong violet emission band was observed at 431 nm for all compositions due to defects such as interface traps existing at the grain boundaries. The weak blue emission band was observed at 460 nm due to intrinsic defects. The weak green emission band was observed at 525 nm and its intensity is found to decrease as the dopant concentration increases which may be due to a decrease in oxygen vacancy concentration (34).

## 5. Conclusions

Nanoparticles of  $Zn_{1-x}Ni_xO$  ( $x = 0, 0.02, 0.04$  and  $0.06$ ) are prepared by chemical precipitation method. XRD analysis reveals the hexagonal wurtzite-type structure and the average crystallite size is predicted to be in the range of 24-35 nm. SEM observations reveals the morphology of the prepared undoped and Ni doped ZnO nanoparticles is found to be flower and Nano rod like structure respectively. EDAX analysis confirms the purity of prepared undoped and Ni doped ZnO nanoparticles. The band gap is blue shifted as Ni concentration increases. The observed red shift in the optical absorption band edge and PL analysis confirms the presence of various point defects of the prepared undoped and Ni doped ZnO nanoparticles.

## References

- [1] Y. M. Hao, S. Y. Lou, S. M. Zhau, R. J. Yuan, G. Y. Zhu, N. Li, *Nanoscale Res. Lett.* **7**, 100 (2012).
- [2] P. M. Shirage, *Materials Today* **16**, 505 (2013).
- [3] N. Goswami, A. Sahai, *Mat. Res. Bull.* **48**, 346 (2013).
- [4] J. Jadhav, M. Patange, S. Biswas, *Carbon Sci. Tech.* **5**, 2 (2013).
- [5] G. Srinet, R. Kumar, V. Sajal, *J. App. Phy.* **114**, 033912 (2013).
- [6] G. Srinet, R. Kumar, V. Sajal, *Cer. Int.* **39**, 7557 (2013).
- [7] Yu-Cheng Chang, *RSC Adv.* **4**, 56241 (2014).
- [8] S. Inbasekaran, R. Senthil, G. Ramamurthy, T. P. Sastry, *Eng Technol* **3**(1), 8601 (2014).
- [9] S. Sabir, M. Arshad, S. K. Chaudhari, 2014, Zinc oxide nanoparticles for revolutionizing agriculture: synthesis and applications.
- [10] A. Shrishti, P. S. Kumar, S. Monika, *Int J Chem Pharma Anal* **1**(3), 141 (2014).
- [11] M.M. Rahman et al. *Journal of Industrial and Engineering Chemistry*, 2014, 20, 1071.
- [12] Xingyan Xu, Chuanbao Cao, *Journal of Magnetism and Magnetic Materials* **377**, 308 (2015).
- [13] Kyung Ho Kimn, Zhuguang Jin, Yoshio Abe, Midori Kawamura, *Materials Letters* **149**, 8 (2015).
- [14] Rana et al., *AIP Advance* **5**, 097118 (2015).
- [15] Y. Kumar, A. K. Rana, P. Bhojane, M. Pusty, V. Bagwe, S. Sen, P. M. Shirage, *Materials Research Express* **2**, 105017 (2015).
- [16] Rana et al. *Applied Surface Science* **379**, 23 (2016).
- [17] Parasharam M. Shirage, Amit Kumar Rana, Yogendra Kumar, Somaditya Sen, S. G. Leonardi, G. Neri, *RSC Adv.* **6**, 82733 (2016).
- [18] Qiaoqiao Yin et al., *RSC Adv.* **6**, 38653 (2016).
- [19] M. Sh. Abdel-Wahab, Asim Jilani, I.SYahia, Attieh A. Al-Ghamdi. *Superlattices and microstructures* **94**, 108 (2016).
- [20] Amit Kumar Rana, Prashant Bankar, Yogendra Kumar, Mahendra A. Dattatray, J. Parasharam, M. Shirage, *RSC Adv.* **6**(106), 104318 (2016)
- [21] R. Saravana Kumar, S. H. S. Dananjaya, Mahanama De Zoysa, Minyang Yang, *RSC Adv.* **6**, 108168 (2016).
- [22] Kun Xu, Changzhen Liu, Rui Chen, Xiaoxiang Fang, Xiuling Wu, Jie Liu, *Physica B* **502**, 155 (2016).
- [23] D. Guruvammal, S. Selvaraj, S. Meenakshi Sundar, *Journal of Alloys and Compounds* **682**, 850 (2016).

- [24] Z. A. Fattah, *Int. J. Eng. Sci. Res. Tech.* **5**(7), 418 (2016).
- [25] Y. Wang et al, *J. Mater. Res.* **31**(15), 15 (2016).
- [26] S. Fabbiyola, V. Sailaja, L. Johnkennedy, M. Bououdina, J. Judith Vijaya, *Journal of Alloys and Compounds* **694**, 522 (2017).
- [27] Umadevi Godavarti, V. D. Mote, Madhavaprasad Dasari, *Modern Electronic Materials* **3**, 179 (2017).
- [28] R. Sankar Ganesh, E. Durgadevi, M. Navaneethan, V. L. Patil, S. Ponnusamy, C. Muthamizhchelvan, S. Kawasaki, P. S. Patil, Y. Hayakawa, *Chemical Physics Letters*, 2017.
- [29] G. Pallavi, Shankar Undre, D. Birajdar, R. V. Kathare, K. M. Jadhav, *Procedia Manufacturing*, 477 (2018)
- [30] Madhava P. Dasari, Umadevi Godavarti, Vishwanath Mote, *Processing and Application of Ceramics* **12**(2), 100 (2018).
- [31] Zahira El khalidi, Bouchaib Hartiti, Maryam Siadat, Elisabetta Comini, Hashitha M. M. Munasinghe Arachchige, Salah Fadili, Philippe Thevenin, *Journal of Materials Science: Materials in Electronics*, 21-March-2019.
- [32] Rajwali Khan, Zulfiqar, Clodoaldo Irineu Levartoski de Araujo, Tahirzeb Khan, Shaukat Ali Khattak, Ejaz Ahmed, Aurangzeb Khan, Burhan Ullah, Gulzar Khan, Kashif Safeen, Akif Safeen, Syed Adnan Raza, *Journal of Materials Science: Materials in Electronics*, 2019.
- [33] Sivanantham Nallusamy, Gopalakrishnan Nammalvar, *Journal of Magnetism and Magnetic Materials* **485**, 297 (2019).
- [34] Prakhar Shuklaa, Jitendra Kumar Shuklab, *Physica B: Condensed Matter* **569**, 31 (2019).